nature climate change

Supplementary information

https://doi.org/10.1038/s41558-024-02057-4

Decadal increases in carbon uptake offset by respiratory losses across northern permafrost ecosystems

In the format provided by the authors and unedited

Table S1. Summary of number of ecosystems used in timeseries analyses of summer (June-August) and annual (12-month) fluxes, parsed by ecosystem (i.e. permafrost presence and biome type).

	Summer Sites		Annual Sites	
Ecosystem	**Tundra**	**Boreal**	**Tundra**	**Boreal**
Permafrost	69	36	15	17
Non-permafrost	18	56	2	36

Table S2. Summary of observations used in time series analyses of summer (June-August) and annual (12-month) fluxes and parsed by longitude and ecosystem (i.e. permafrost presence and biome type).

Flux	Full dataset	North America	Eurasia	2003-present
Summer NEE				
Permafrost	386	261	125	350
Non-permafrost	286	140	146	225
Summer GPP				
Permafrost	277	204	73	254
Non-permafrost	250	135	115	204
Summer R_{eco}				
Permafrost	296	219	77	269
Non-permafrost	264	137	127	208
Annual NEE				
Permafrost	94	75	19	86
Non-permafrost	208	106	102	159
Annual GPP				
Permafrost	72	62	10	64
Non-permafrost	164	86	78	128
Annual R_{eco}				
Permafrost	73	62	11	65
Non-permafrost	185	95	90	145

Table S3. Summary of timeseries analyses results from models run on datasets subset from 2003-present.

Ecosystem Flux	Annual Changes 2003-Present			Summer Changes 2003-Present		
	Slope (SE)	R^2_{cond}	*P*	Slope (SE)	R^2_{cond}	*P*
NEE						
Permafrost	1.0 (1.6)	0.51	0.54	-1.9 (1.3)	0.78	0.13
Non-Permafrost	-4.3 (1.8)	0.76	0.02	-4.1 (1.3)	0.80	0.002
GPP						
Permafrost	-5.8 (3.2)	0.85	0.08	-3.4 (2.6)	0.76	0.20
Non-Permafrost	-13.22 (9.6)	0.93	0.17	convergence failure		
R_{eco}						
Permafrost	6.2 (3.7)	(0.78)	0.10	2.91 (1.2)	0.84	0.02
Non-Permafrost	convergence failure			convergence failure		

Because the number of sites collecting data has increased since the beginning of our time series, we re-ran our models on a subset of the data to assess the robustness of our findings to temporal biases in data collection. We re-ran the models on the subset of observations from 2003-present, representing the most recent 20 years of data. This represents 85% and 81% of summer and annual NEE estimates, 87% and 74% of summer and annual GPP, and 85% and 81% of summer and annual Reco estimates, respectively. This analysis supported our core conclusion that annual CO2 uptake is increasing across non-permafrost ecosystems (P = 0.02), but not across permafrost ecosystems (P = 0.54), with estimates of both slopes within 1 g m-2 yr-1 of estimates based on the full dataset (Fig. 2 in main text). Long-term trends in summer NEE were also largely similar when using the shortened timeseries, although the non-permafrost ecosystem C sink increased at a slightly faster rate (-4.1 g m-2 yr-1; P = 0.002 vs. -2.6 in full dataset), and at a slightly slower rate in permafrost ecosystems (-1.9 g m-2 yr-1; P = 0.13 vs. -3.0 in full dataset), with 95% confidence intervals in the slopes of both ecosystems largely overlapping between the subset and full datasets. Analysis of changes in the component fluxes across this shorter time period supported the idea of increased amplification rates of permafrost C cycling, with both GPP and Reco generally increasing. Conversely, in non-permafrost sites (where we detected no significant trends in GPP and Reco in the full dataset), this shortened window of observations led to no consistent trends in these component fluxes, with models often failing to converge.

Table S4. Summary of annual timeseries analyses results with datasets subset by landmass (i.e. North America and Greenland vs. Eurasia).

	North America			***Eurasia***		
	Slope (SE)	**R^2_{cond}**	***P-value***	**Slope (SE)**	**R^2_{cond}**	***P-value***
NEE						
Permafrost	3.4 (1.7)	0.46	<0.05	-1.9 (6.8)	0.79	0.79
Non-Permafrost	-0.1 (2.8)	0.66	0.97	-8.6 (4.1)	0.86	0.04
GPP						
Permafrost	-6.8 (3.2)	0.89	0.04	-13.0 (13.2)	0.94	0.37
Non-Permafrost	1.7 (8.5)	0.78	0.84	-12.9 (6.7)	0.98	0.06
R_{eco}						
Permafrost	7.3 (3.6)	0.79	<0.05	16.1 (8.5)	0.96	0.12
Non-Permafrost	convergence failure			3.19 (5.6)	0.95	0.57

To assess the effect of broad-scale spatial patterns in data collection on our results, we subset our data by landmass, and re-ran the models for North America (including Greenland) and Eurasia. North America (largely Alaska) represents 82% of our annual observations of permafrost NEE (Table S2), and here, we found that the trend of increasing annual NEE (i.e. weakening land CO2 sink over time; Fig. 2b main text) became statistically significant. Similarly, evidence was stronger for increasing annual R^{eco} across North American permafrost ecosystems ($P < 0.05$). Notably, the changes in both GPP and Reco across Eurasian permafrost ecosystems were roughly double those observed in North America, perhaps suggesting a greater amplification of annual C cycling in Eurasia, but the very limited sample size of annual permafrost fluxes here (Table S2) strongly limits interpretation of these results. While trends in permafrost sites may be driven by North American ecosystems, the trends we observed across non-permafrost sites appeared to be stronger in Eurasia. The increased annual CO2 uptake (decreasing NEE) in non-permafrost ecosystems was statistically significant in Eurasia ($P = 0.04$), where we found evidence for increased annual GPP over time ($P = 0.06$), but no clear trend in annual R_{eco}. In contrast, we found little evidence for consistent trends in NEE, GPP, or R_{eco} in North American non-permafrost ecosystems.

Table S5. Comparison of slopes and 95% confidence intervals derived from frequentist models (reported in main text), with slopes and 95% credible intervals derived from Bayesian reanalysis. Model root mean square errors (RMSE) for frequentist models are shown in comparison to RMSEs recalculated using cluster-level leave-one-out cross validation (LOOCV). The differences in between model RMSE and cross-validated RMSE are reported in the last column in units of percent change.

Model	Model Slope (CI)	Bayesian Slope (CI)	Model RMSE	LOOCV RMSE	Difference in RMSE (%)
Annual NEE Permafrost	1.67 (-1.4 – 4.73) P = 0.28	1.25 (-0.87 — 3.38) P = 0.52	71	79	12
Annual NEE Non-Permafrost	-4.81 (9.65 – 0.04) P =0.05	-5.75 (-8.07 – -3.4) P < 0.001	125	120	-4
Annual GPP Permafrost	-6.30 (-12.07 – -0.47) P = 0.03	-5.5 (-9.38 – -1.62) P = 0.03	217	246	13
Annual GPP Non-Permafrost	-6.71 (-18.08 – 4.65) P = 0.24	-10.2 (-16.18 – -4.18) P = 0.004	433	513	18
Annual Reco Permafrost	6.08 (-0.37 – 12.53) P = 0.06	6.03 (1.76 – 10.28) P = 0.02	200	NA	NA
Annual Reco Non-permafrost	4.16 (-4.97 – 13.28) P = 0.37	4.05 (-1.32 – 9.45) P = 0.34	409	NA	NA
Summer NEE Permafrost	-3.04 (-4.67 – -1.42) P < 0.001	-2.47 (-3.57 – -1.37) P < 0.001	79	77	-2
Summer NEE Non-permafrost	-2.6 (-4.41 – -0.8) P = 0.005	-2.34 (-3.59 – -1.09) P = 0.001	104	96	-8
Summer GPP Permafrost	-6.8 (-10.92 – -2.69) P = 0.001	-5.44 (-7.88 – -2.98) P < 0.001	167	166	-1
Summer GPP Non-Permafrost	-1.64 (-8.24 – 4.96) P = 0.62	-3.02 (-6.32 – 0.32) P = 0.21	257	NA	NA
Summer Reco Permafrost	3.08 (0.93 – 5.23) P = 0.005	2.73 (1.23 – 4.24) P = 0.002	126	NA	NA
Summer Reco Non-Permafrost	0.78 (-3.93 – 5.48) P = 0.75	0.53 (-2.07 – 3.12) P = 0.93	216	NA	NA

To further assess the uncertainty in the slope estimates of our timeseries models, we refit all models (with an identical random effects and autocorrelation structure) in a Bayesian framework using the brms package in R. We assigned the fixed effect parameters from the frequentist model outputs as prior distributions, with relatively uninformative priors for the random effects and covariance parameters (Student's T (ν=3, μ=0, σ=47) and LKJ η=1, respectively). Each timeseries model was run on 8 separate MCMC chains of 20,000 steps with a warmup of 12,000, resulting in 64,000 total samples in the posterior distribution. We then compared the slopes and 95% credible intervals from this distribution to the slopes and confidence intervals derived from the original frequentist models. We calculated P-values for the Bayesian slopes as the density value of posterior distribution at the null (0) divided by the density at the Maximum A Posteriori value for the slope (Mills 2019). Generally, the frequentist and Bayesian analyses agreed, with significant (or marginally significant) slopes based on one approach corresponding to significant slopes using the other approach. The only exception to this was the trend towards increasing annual GPP in non-permafrost systems, which was not statistically significant in our original

analysis (slope = -6.7 g m-2 yr-1, P=0.25), but had a steeper slope that differed from zero based on the Bayesian analysis (slope = -10.2, P=0.004).

Because our analyses included a relatively small number of sites, the inclusion (or exclusion) of single sites may affect the conclusions of our models. We assessed the robustness of our findings using leave-one-out cross validation (LOOCV) based on cluster-wise exclusion using the cv package in R85. Briefly, for each timeseries model we iteratively removed one site at a time and recalculated the model to assess its predictive ability for the observations in the removed cluster86. We then compared the root mean squared error (RMSE, calculated using fixed effects) based on the predictions to the RMSE for the original model. This analysis suggested that our conclusions regarding NEE trends were likely robust to biases in site selection: The predictive RMSE based on LOOCV was lower than the model based RMSE for the models where we detected a significant trend (permafrost and non-permafrost summer NEE, annual non-permafrost NEE; Table S5). In contrast, GPP and Reco trends appeared to be more sensitive to removing sites. It was not possible to calculate the LOOCV RMSE for many of these models, because running the models on one or more of the subsets of data resulted in models failing to converge. In cases when GPP and Reco models converged for all subsets of data, the predictive RMSE was generally higher than that of the original model. The one exception to this was the model showing an increase in summer GPP in permafrost sites, where the predictive RMSE based on LOOCV was slightly smaller (1%, Table S5) than the original model. Collectively, these uncertainty analyses point to a greater degree of confidence in NEE timeseries than in GPP or Reco. This is perhaps not surprising, given that we have a larger sample size for NEE (Table S2). Additionally, is the variable measured NEE at these sites (using eddy covariance towers or chambers), while GPP and Reco are estimated by partitioning the NEE flux, which introduces additional uncertainty into these estimates.

Table S6. Slopes (± standard error) for decadal changes in CO_2 flux by month in permafrost and non-permafrost ecosytems.

Month	Permafrost Presence	Change in NEE ($g\ C\ m^{-2}\ yr^{-1}$)	Change in GPP ($g\ C\ m^{-2}\ yr^{-1}$)	Change in R_{eco} ($g\ C\ m^{-2}\ yr^{-1}$)
Jan	Nonpermafrost	0.06 ± 0.09 (P = 0.51, n=201)	0.42 ± 0.19 (P = 0.03, n=163)	-0.4 ± 0.24 (P = 0.11, n=177)
Jan	Permafrost	0.05 ± 0.18 (P = 0.76, n=110)	0.21 ± 0.2 (P = 0.31, n=69)	0.05 ± 0.25 (P = 0.83, n=77)
Feb	Nonpermafrost	0 ± 0.09 (P = 0.98, n=194)	0.13 ± 0.36 (P = 0.72, n=166)	-0.06 ± 0.35 (P = 0.85, n=176)
Feb	Permafrost	0.12 ± 0.13 (P = 0.37, n=117)	0.12 ± 0.1 (P = 0.23, n=73)	0.16 ± 0.14 (P = 0.25, n=80)
Mar	Nonpermafrost	-0.12 ± 0.15 (P = 0.44, n=206)	-0.12 ± 0.22 (P = 0.59, n=173)	0.13 ± 0.15 (P = 0.40, n=182)
Mar	Permafrost	0.24 ± 0.14 (P = 0.09, n=142)	0.21 ± 0.2 (P = 0.3, n=84)	0.47 ± 0.24 (P = 0.06, n=91)
Apr	Nonpermafrost	-0.09 ± 0.2 (P = 0.64, n=225)	0.1 ± 0.36 (P = 0.79, n=196)	-0.19 ± 0.2 (P = 0.35, n=195)
Apr	Permafrost	-0.06 ± 0.16 (P = 0.70, n=167)	-0.23 ± 0.27 (P = 0.39, n=99)	0.21 ± 0.24 (P = 0.38, n=102)
May	Nonpermafrost	-0.06 ± 0.3 (P = 0.84, n=235)	-0.48 ± 0.6 (P = 0.43, n=202)	0.35 ± 0.36 (P = 0.34, n=206)
May	Permafrost	-0.34 ± 0.19 (P = 0.07, n=267)	-0.89 ± 0.41 (P = 0.03, n=163)	0.45 ± 0.29 (P = 0.13, n=183)
Jun	Nonpermafrost	-0.66 ± 0.36 (P = 0.07, n=260)	-0.55 ± 0.78 (P = 0.48, n=224)	-0.07 ± 0.52 (P = 0.90, n=238)
Jun	Permafrost	-0.73 ± 0.29 (P = 0.01, n=315)	-1.5 ± 0.57 (P = 0.009, n=225)	0.58 ± 0.35 (P = 0.10, n=241)
Jul	Nonpermafrost	-1.06 ± 0.35 (P = 0.003, n=266)	-1.68 ± 0.75 (P = 0.03, n=230)	0.22 ± 0.65 (P = 0.73, n=245)
Jul	Permafrost	-1.12 ± 0.38 (P = 0.003, n=353)	-2.12 ± 0.72 (P = 0.004, n=259)	1.05 ± 0.42 (P = 0.01, n=278)
Aug	Nonpermafrost	-0.42 ± 0.29 (P = 0.15, n=269)	-0.32 ± 0.66 (P = 0.62, n=233)	-0.27 ± 0.61 (P = 0.65, n=248)
Aug	Permafrost	-0.72 ± 0.32 (P = 0.03, n=353)	-2.46 ± 0.62 (P < 0.001, n=247)	1.52 ± 0.37 (P < 0.001, n=271)
Sep	Nonpermafrost	0.32 ± 0.2 (P = 0.10, n=242)	0.08 ± 0.41 (P = 0.84, n=221)	0.35 ± 0.42 (P = 0.40, n=225)
Sep	Permafrost	-0.11 ± 0.32 (P = 0.73, n=282)	-1.39 ± 0.55 (P = 0.01, n=183)	1.12 ± 0.39 (P = 0.005, n=196)
Oct	Nonpermafrost	-0.17 ± 0.17 (P = 0.32, n=221)	-0.35 ± 0.18 (P = 0.05, n=205)	0.21 ± 0.29 (P = 0.45, n=206)
Oct	Permafrost	0.35 ± 0.15 (P = 0.02, n=203)	-0.05 ± 0.13 (P = 0.7, n=118)	0.61 ± 0.2 (P = 0.003, n=131)
Nov	Nonpermafrost	0.28 ± 0.14 (P = 0.04, n=209)	-0.03 ± 0.12 (P = 0.79, n=185)	0.31 ± 0.19 (P = 0.10, n=195)
Nov	Permafrost	0.33 ± 0.13 (P = 0.01, n=143)	-0.02 ± 0.11 (P = 0.88, n=77)	0.48 ± 0.23 (P = 0.04, n=82)
Dec	Nonpermafrost	0.09 ± 0.12 (P = 0.46, n=200)	-0.16 ± 0.15 (P = 0.27, n=174)	0.3 ± 0.19 (P = 0.12, n=182)
Dec	Permafrost	0.61 ± 0.17 (P = 0.001, n=129)	0.09 ± 0.12 (P = 0.49, n=75)	0.6 ± 0.21 (P = 0.006, n=79)

Table S7. Summary of number of ecosystems used in meta-regressions of air temperature effects on summertime (June-August) fluxes, parsed by permafrost presence, biome type, and soil C:N ratio.

	Permafrost	**Non-permafrost**	**Tundra**	**Boreal**
Tundra	NEE = 20 GPP = 16 R_{eco} = 17	NEE = 2 GPP = 2 R_{eco} = 2		
Boreal	NEE = 7 GPP = 7 R_{eco} = 7	NEE = 18 GPP = 18 R_{eco} = 18		
N limited (C:N ≥ 15)	NEE = 19 GPP = 17 R_{eco} = 18	NEE = 14 GPP = 14 R_{eco} = 14	NEE = 17 GPP = 15 R_{eco} = 16	NEE = 16 GPP = 16 R_{eco} = 16
N rich (C:N < 15)	NEE = 8 GPP = 6 R_{eco} = 6	NEE = 6 GPP = 6 R_{eco} = 6	NEE = 5 GPP = 3 R_{eco} =3	NEE = 9 GPP = 9 R_{eco} = 9

Figure S1. Maps of datasets used for each analysis. Green dots represent sites with at least one monthly flux included in timeseries analysis of monthly change over time. Purple dots represent sites with at least one full summer (sum of June, July, and August) included in summer timeseries analysis. Red dots represent sites with at least one full year (12 monthly fluxes) included in annual timeseries analysis. Yellow sites contain at least five years of summer fluxes and were included in metaregression analysis.

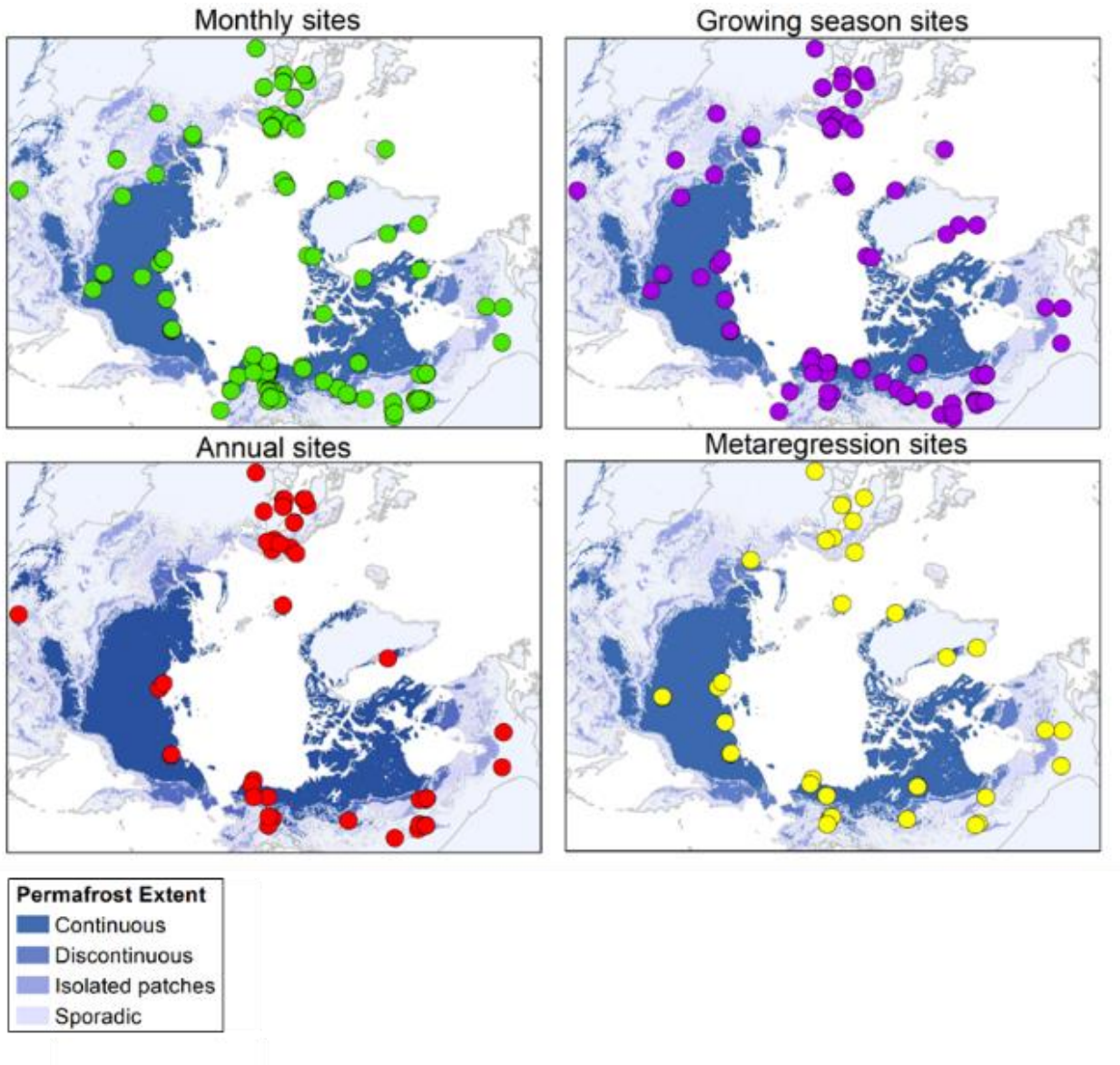

Figure S2. Top panel: Slopes from linear mixed-effects models showing decadal changes in summer (June-August) and annual net ecosystem exchange (NEE) across high latitude ecosystems (identical to Fig 2 in main text, but with observations shown as points). **Bottom panel:** Residuals from linear mixed-effects models of decadal changes in NEE, GPP, and R_{eco}.